

R/V Shinsei-maru Cruise Report
KS-19-22

Interaction between TWC front and internal gravity
waves in the central Japan Sea: Detailed observations
of turbulent mixing and primary production

Area Off Noto Peninsula and Sado Island
Oct. 25 – 31. 2019

Joint Usage/Research Center for Atmosphere and
Ocean Science (JURCAOS)
Japan Agency for Marine-Earth Science and
Technology (JAMSTEC)

2. Research Proposal and Science Party

- Title of proposal:
Overall: Interaction between TWC front and internal gravity waves in the central Japan Sea:
Detailed observations of turbulent mixing and primary production
- Representative of Science Party [Affiliation]: Yusuke Kawaguchi [Atmosphere and Ocean Research Institute (AORI), The University of Tokyo]
- Science Party (List) [Affiliation, assignment, etc.]
Yusuke Kawaguchi [AORI]: Overall
Taku Wagawa [Fisheries Research Agency: (FRA)]: CTD*, VMP
Daiki Ito [FRA]: SADCP*, XCTD*, VMP
Tomoharu Senju [Research Institute for Applied Mechanics, Kyushu University (RIAM)]: CTD, VMP
Itsuka Yabe [AORI]: SVP*, LADCP*, VMP
Akie Sakai [RIAM]: CTD, VMP
Kazuki Horio [Graduate School of Fishery Science, Hokkaido University (HU)]: CTD, VMP
Koshiro Taya [HU]: CTD, VMP
Yohei Katayama [Marine Works Japan (MWJ)]: CTD, VMP
Asterisks (*) represents principal investigators of activities.

3. Research/Development Activities

3.1. CTD

(1) Personnel

Taku Wagawa: FRA, principal investigator
Yusuke Kawaguchi, Itsuka Yabe: AORI
Daiki Ito: FRA
Tomoharu Senjyu, Akie Sakai: RIAM
Kazuki Horio, Koshiro Taya: Hokkaido University

(2) Objectives

CTD measurements aim to capture mesoscale hydrographic structures of the Tsushima Warm Current and eddies formed around flows.

(3) Instruments and methodology

Along YR-line, E-line, and SI-line CTD measurements were made to 1000 dbar or the bottom. Water samples were also taken along SI-line to calibrate salinity, dissolved oxygen, and chlorophyll-*a*. Part of the samples at each depth was reserved for nutrient analysis (NO₃ and PO₄).

(4) CTD deployment positions

Stn	Date	Time (JST)	Lat (deg)	Lat (min)	Lon (deg)	Lon (min)
YR09	20191025	2218	37	31.5820	135	52.8143
YR08	20191026	0021	37	24.5400	135	56.9100
YR07	20191026	0204	37	17.2700	136	00.8500
YR06	20191026	0357	37	10.6700	136	05.1600
YR05	20191026	0538	37	03.6500	136	08.7000
YR04	20191026	0707	36	57.0300	136	12.6700
YR03	20191026	0839	36	50.4160	136	16.9645
YR02	20191026	1007	36	43.7774	136	20.2513
YR01	20191026	1121	36	38.0472	136	23.4763
YR10	20191026	1825	37	41.0000	135	48.0000
YR11	20191026	2035	37	51.4463	135	41.6252
E09	20191027	0058	37	58.5100	135	58.5100
E08	20191027	0507	38	06.1700	136	15.9000
E07	20191027	0910	38	13.7060	136	32.5018
E06	20191027	1330	38	21.3500	136	49.8400
E05	20191027	1731	38	28.5800	137	07.1100
E04	20191027	1204	38	36.4864	137	24.1605
E03	20191028	0121	38	43.9200	137	41.2800
E02	20191028	0509	38	51.7200	137	58.4400
E01	20191028	0907	38	59.2066	138	15.4341
SI06	20191028	1721	39	20.0100	137	24.7800
SI05	20191028	2135	39	05.1536	137	34.7587
SI04	20191029	0157	38	50.3400	137	45.0100
SI03	20191029	0524	38	35.0700	137	55.2400
SI02	20191029	0954	38	20.9911	138	05.7013
SI01	20191029	1356	38	08.6800	138	13.1700
FATO1	20191030	0643	38	40.1900	137	51.8600
FATO2	20191031	0240	38	40.6165	137	52.4331

(5) Preliminary Results

Vertical cross-sections of potential temperature, salinity, and geostrophic velocities conveniently characterized details of the water properties around the mesoscale frontal/eddy structures (Fig. 3.1.1). YR/SI-line and E-line were characterized, respectively, by cyclonic eddy and a vortex pair. Their structures were apparent within the upper 250 dbar. Warm ($\sim 20^{\circ}\text{C}$) and low-salinity (< 34.0) water extended from the sea surface to about 50 dbar. Below the sea-surface water, the Tsushima Warm Current Water with a potential temperature $> 10^{\circ}\text{C}$ and salinity > 34.2 were observed. Although the vertical velocity structures

were more intense at the surface, strong flows $> 0.10 \text{ m s}^{-1}$ were found down to 200 dbar.

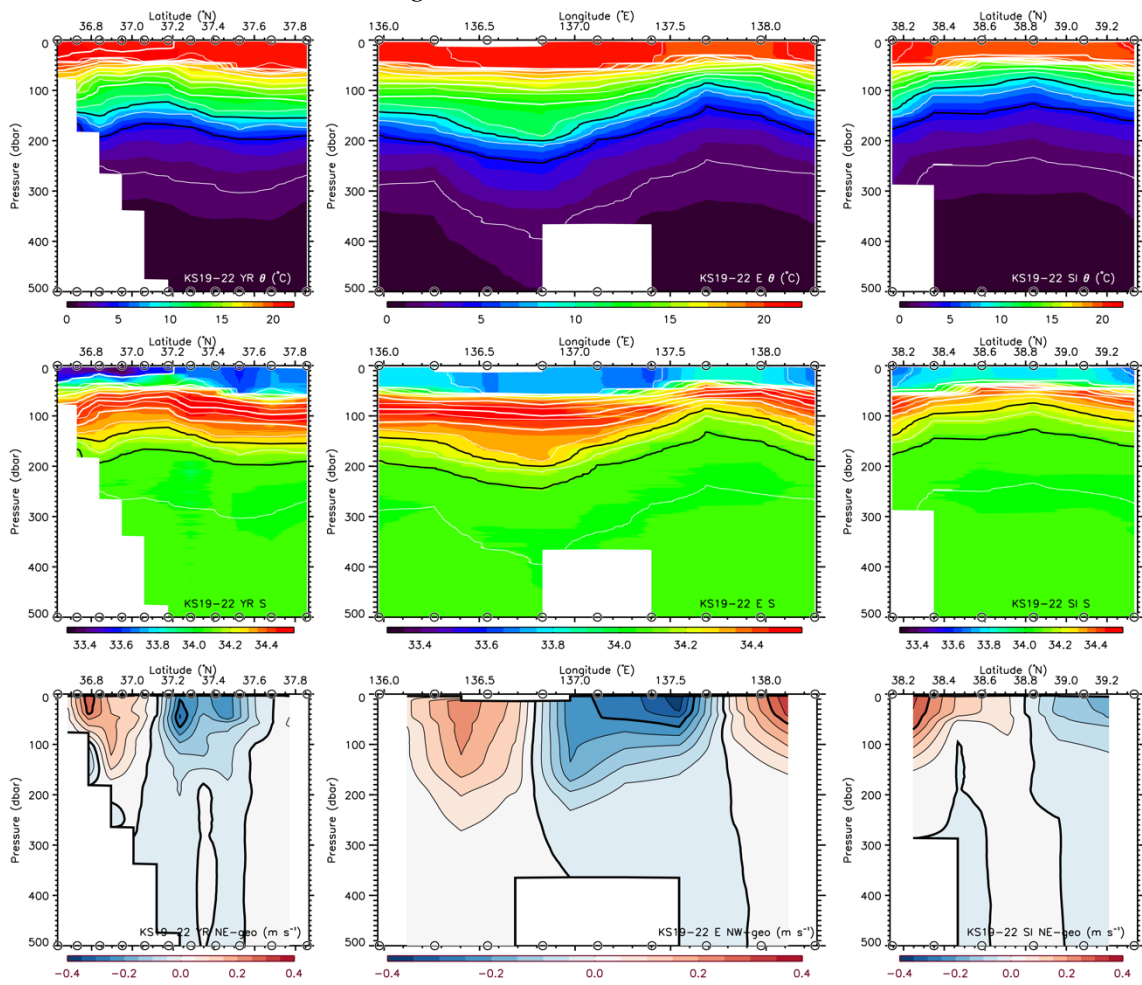


Figure 3.1.1 Vertical cross-sections of (top) potential temperature, (middle) salinity, (bottom) geostrophic velocity along (left) YR-line, (center) E-line, and (right) SI-line. Top and middle panels: thin and thick contours respectively show potential density at intervals of $\sigma_{\theta}=0.25 \text{ kg m}^{-3}$ and $\sigma_{\theta}=0.5 \text{ kg m}^{-3}$. Thick black contours show the isopycnals corresponding to $\sigma_{\theta}=26.5$ and 27.0 kg m^{-3} . Bottom panels: positive velocities indicate the northeastward (northwestward) flows perpendicular to YR-line and SI-line (E-line).

3.2. VMP

(1) Personnel

Yusuke Kawaguchi: AORI, principal investigator

Itsuka Yabe: AORI

Taku Wagawa, Daiki Ito: FRA

Tomoharu Senjyu, Akie Sakai: RIAM

Kazuki Horio, Koshiro Taya: Hokkaido University

(2) Objectives

Direct microstructure measurements with a quasi-free-falling instrument VMP-250 were repeatedly

performed during KS-19-22. This aims to assess turbulent kinetic energy and diffusivity in the water, which are often explained by some larger scale physical phenomena such as geostrophic balanced motion, internal waves, mesoscale features, and so on.

(3) Instruments and methodology

Regarding the microstructure observations, the VMP-250 (Rockland Science, Inc.) was utilized. The device is loosely tethered from a winch, that is installed on the side deck, and makes it possible the quasi-free-falling under only little tension on the line. A couple of fast shear sensors and a single fast temperature sensor (FP07) are installed on the tip of instrument's main body, which collect respectively vertical current shear and vertical temperature gradient at a constant frequency of 512 Hz. The current shear was preliminarily processed by using prepared Matlab programs (ODAS ver. 4.3) to give totally 48 vertical profiles of turbulent kinetic energy diffusivity rate, ϵ , in terms of pressure. The successive profiling of VMP measurements underwent at the sections of Line E and Line SI. VMP profiling was also performed on the hour throughout the stationary observation campaign at the FATO station, lasting for more or less 18 hours.

(4) VMP deployment positions

Stn.	Cast #	Month	Day	Start time (JST)		End time (JST)		Latitude		Longitude		File #
				Hour	Min	Hour	Min	Degree	Min	Degree	Min	
Line E												
Em09	1	10	26	22	33	22	47	37	55.7	135	50.1633	87
E09	1	10	27	0	11	0	25	37	58.833	135	58.6603	88
Em08	1	10	27	2	55	3	9	38	2.604	136	7.233	89
E08	1	10	27	4	25	4	40	38	6.1881	136	15.914	90
Em07	1	10	27	7	3	7	17	38	10.192	136	23.214	91
E07	1	10	27	8	29	8	44	38	13.9792	136	32.848	92
Em06	1	10	27	11	20	11	35	38	17.4811	136	41.3943	93
E06	1	10	27	12	42	12	56	38	21.4236	136	49.8623	94
Em05	1	10	27	15	34	15	48	38	25.1879	136	58.4806	95
E05	1	10	27	16	56	17	5	38	28.9611	137	7.0952	96
Em04	1	10	27	19	0	19	14	38	32.6215	137	15.7451	97
E04	1	10	27	20	21	20	35	38	36.4866	137	24.2303	98
Em03	1	10	27	23	1	23	16	38	40.1684	137	32.677	99
	2	10	27	23	25	23	34	38	39.6003	137	33.0896	99
E03	1	10	28	0	42	0	56	38	44.0729	137	41.2091	100
Em02	1	10	28	3	5	3	19	38	47.8597	137	49.7513	101
E02	1	10	28	4	26	4	40	38	51.5957	137	58.3404	102

Em01	1	10	28	7	6	7	20	38	55.3444	138	6.8637	103
E01	1	10	28	8	25	8	40	38	59.179	138	15.4166	104
Line SI												
SIm06	1	10	28	15	3	15	17	39	20.0498	137	17.7908	106
SI06	1	10	28	16	43	16	57	39	19.9511	137	24.8181	107
SIm05	1	10	28	19	27	19	41	39	11.8377	137	30.0114	108
SI05	1	10	28	20	54	20	9	39	5.0694	137	34.9543	109
SIm04	1	10	28	23	46	23	0	38	57.516	137	40.3431	110
SI04	1	10	29	1	17	1	32	38	50.128	137	45.2035	111
SI03	1	10	29	4	43	4	57	38	34.9867	137	55.3177	112
SIm02	1	10	29	7	31	7	15	38	27.9773	137	0.2166	113
SI02	1	10	29	9	14	9	28	38	20.0823	137	5.5517	114
SIm01	1	10	29	12	1	12	15	38	14.3477	137	9.7413	115
SI01	1	10	29	13	24	13	30	38	8.8305	137	13.2687	116
FATO												
FATO	1	10	30	9	0	9	14	38	40.1836	137	51.785	123
FATO	2	10	30	10	0	10	14	38	40.1774	137	51.77	124
FATO	3	10	30	11	0	11	14	38	40.1819	137	51.777	125
FATO	4	10	30	12	0	12	14	38	40.1894	137	51.7925	126
FATO	5	10	30	13	0	13	14	38	40.1809	137	51.7997	127
FATO	6	10	30	14	0	14	14	38	40.1865	137	51.7856	128
FATO	7	10	30	15	0	15	14	38	40.1864	137	51.8004	129
FATO	8	10	30	16	0	16	14	38	40.1927	137	51.7971	130
FATO	9	10	30	17	0	17	14	38	40.1901	137	51.7955	131
FATO	10	10	30	18	0	18	14	38	40.1935	137	51.791	132
FATO	11	10	30	19	0	19	14	38	40.1903	137	51.7938	133
FATO	12	10	30	20	0	20	14	38	40.1923	137	51.7921	134
FATO	13	10	30	21	0	21	14	38	40.1894	137	51.7828	135
FATO	14	10	30	22	0	22	14	38	40.1944	137	51.7762	136
FATO	15	10	30	23	0	23	14	38	40.1932	137	51.784	137
FATO	16	10	31	0	0	0	14	38	40.2031	137	51.8025	138
FATO	17	10	31	1	0	1	14	38	40.2006	137	51.8416	139
FATO	18	10	31	2	0	2	14	38	40.2141	137	51.8711	142

(5) Preliminary Results

Overall, the VMP data show the existence of increased dissipation rate, being the magnitude of $\varepsilon = O(10^{-3}) \text{ W kg}^{-1}$, at the depth of upper 50 m of water column, which is generally coincident with the depth of

surface mixed layer. Those signals are suggestive of the direct mixing due to surface winds or breaking of surface waves. Also, it suggests that the wind-driven turbulent kinetic energy is vertically transported and make it fully energetic over the SML depth.

During the stationary observation at the FATO mooring site, time evolution of hydrographic and turbulence variables were depicted (Fig. 3.2.3). Over the 18 h observation, the basic structure of sea water remain unchanged; it is covered by ~40 m SML at the top, characterized by warm (~28 °C) and low saline (~33.8) water. Intriguingly, at hours between 17:00 and 22:00, the stratified interface at the SML bottom experienced an intriguing move with heaving and vertical separation. The density field (contours) and buoyancy frequency (middle panel) clearly documents the temporal evolution. It appears on the dissipation rates from shear 1 and shear 2 as certain elevation, being $\varepsilon = O(>10^{-8}) \text{ W kg}^{-1}$.

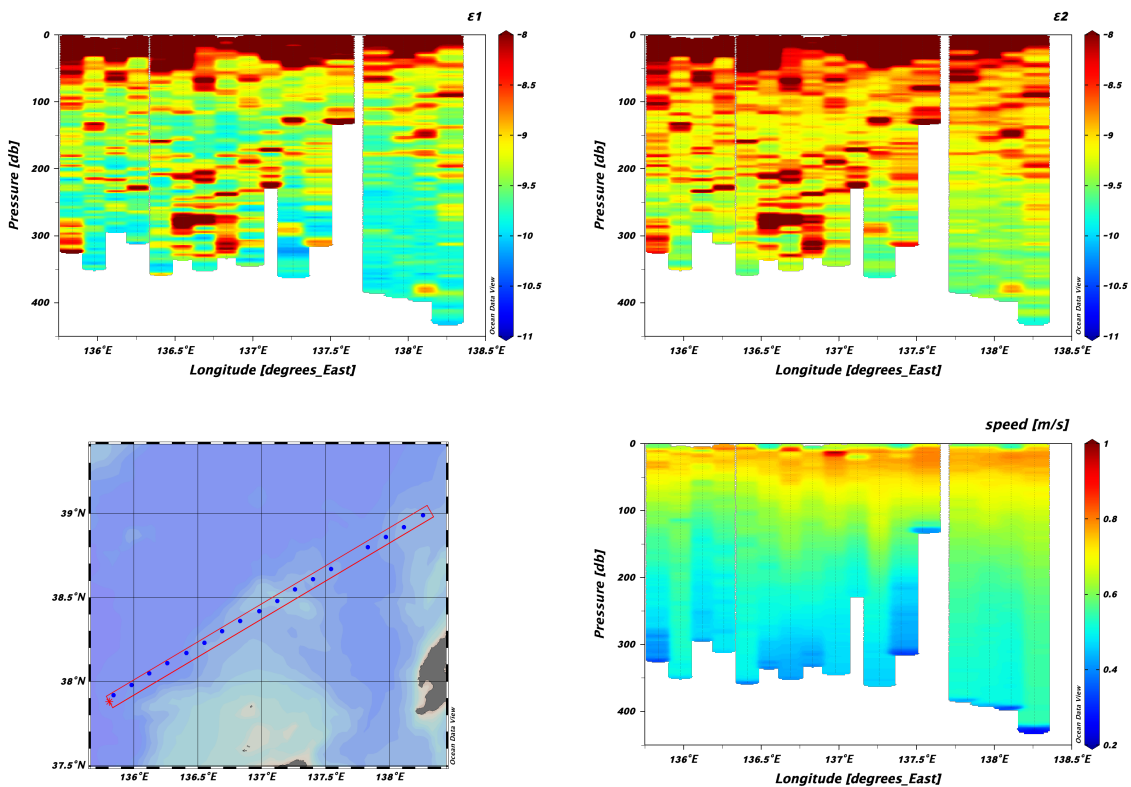


Figure 3.2.1 Vertical section of ε on Line E calculated from sensors of (top left) shear 1 and (top right) shear 2. Bottom panels: (left) positions of observations and (left) falling speed on Line E.

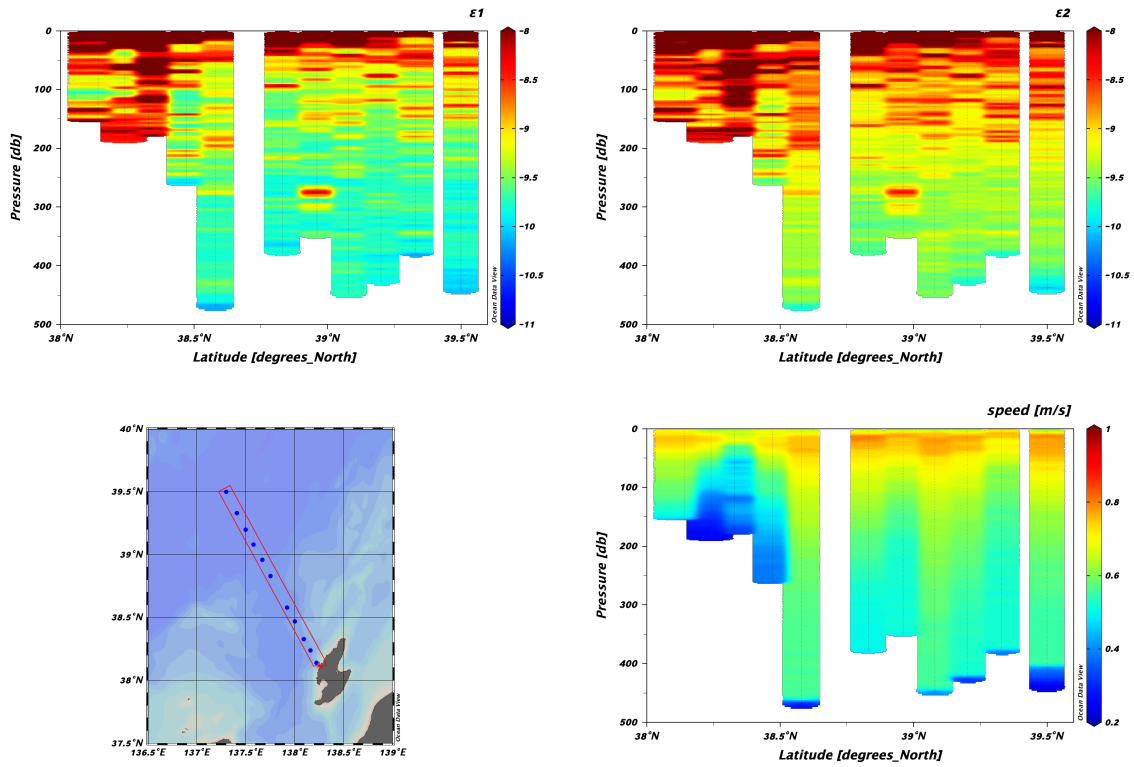


Figure 3.2.2 Same as Fig. 3.2.1 but for Line SI.

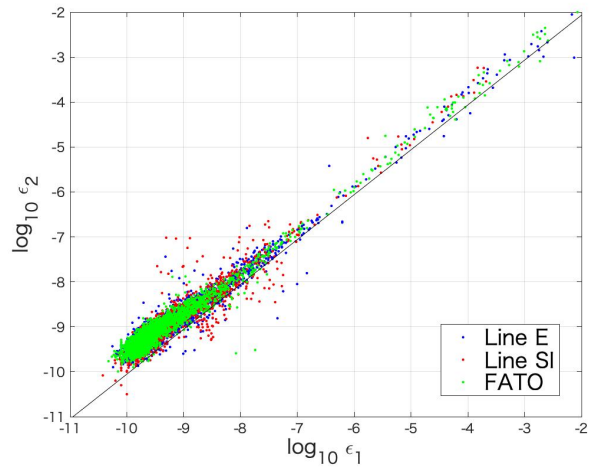


Figure 3.2.4 Comparison of calculated ϵ values between shear 1 and shear 2 for the VMP data taken at Line E (blue), Line SI (red), and FATO (green).

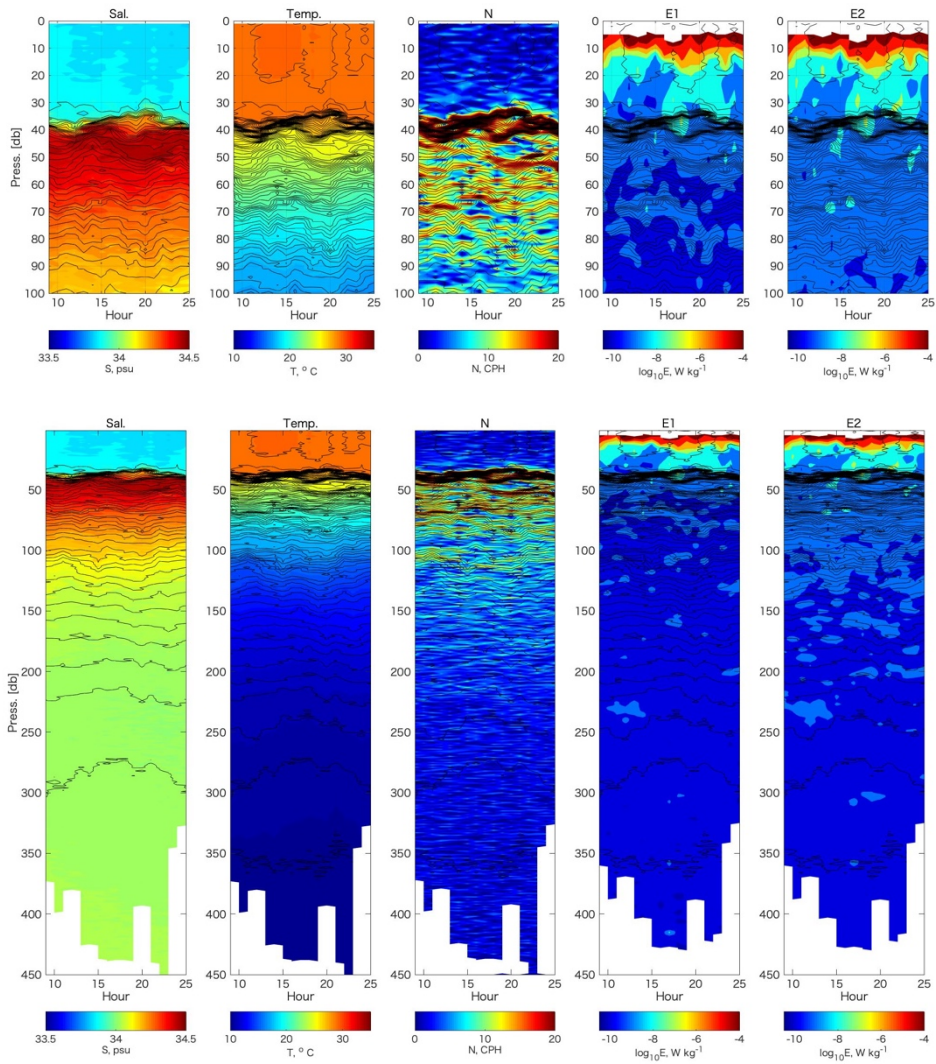


Figure 3.2.3 Results from a stationary observation at the FATO site: salinity, temperature, buoyancy frequency, the dissipation rate ε . Right two panels, ε_1 and ε_2 , show respectively ε from Shear 1 and Shear 2 sensors. Top lines panels enlarge the signature at top 100 m.

In Fig. 3.2.4, the comparison of calculated ε values from sensors between shear 1 (SN = 965) and shear 2 (SN = 960) are shown. Distribution of scattering dots represents the shear 2 sensor is somewhat more sensitive compared to that from shear 1. That difference is roughly estimated by a factor of two or greater. That inconsistency appears the most manifest as it is in the least energy level of turbulence being $\varepsilon = O(10^{-10}) \text{ W kg}^{-1}$. That difference might be responsible for the sensitivity limitation of each sensor, that perceives the electric noise. Otherwise, any correction would be required. It could suggest a formation of Kelvin-Helmholtz billow and an overturning event.

3.3 LADCP

(1) Personnel

Itsuka Yabe: AORI, principal investigator

Yusuke Kawaguchi: AORI

Taku Wagawa, Daiki Ito: FRA

Tomoharu Senjyu, Akie Sakai: RIAM

Kazuki Horio, Koshiro Taya: Hokkaido University

(2) Objectives

LADCP measurements were conducted to examine the jet structures of Tsushima Warm Current and vertical structures of anti-cyclonic and cyclonic eddies.

(3) Instruments and methodology

The Work Horse 300 kHz ADCP manufactured by Teledyne RD Instruments was used. The ADCP was installed in the frame of CTD and set to downward looking. The first bin depth and the bin interval were set at 1.76 m below the instrument and 4 m, respectively. The three lines across the TWC jet and eddies were observed for the KS19-22 cruise: YR-line, E-line and SI-line. LADCP measurements were conducted from the surface to the bottom (or 1000 m) at each station. Velocity profiles were derived using the method of Visbeck (2002). Only the shear components were derived where the water depth at the station was greater than 1000 m. Velocity data were adjusted with the reference depth at 500 m.

(4) LADCP deployment positions

Stn	Date	Time (JST)	Lat (deg)	Lat (min)	Lon (deg)	Lon (min)
YR09	20191025	2218	37	31.5820	135	52.8143
YR08	20191026	0021	37	24.5400	135	56.9100
YR07	20191026	0204	37	17.2700	136	00.8500
YR06	20191026	0357	37	10.6700	136	05.1600
YR05	20191026	0538	37	03.6500	136	08.7000
YR04	20191026	0707	36	57.0300	136	12.6700
YR03	20191026	0839	36	50.4160	136	16.9645

YR02	20191026	1007	36	43.7774	136	20.2513
YR01	20191026	1121	36	38.0472	136	23.4763
YR10	20191026	1825	37	41.0000	135	48.0000
YR11	20191026	2035	37	51.4463	135	41.6252
E09	20191027	0058	37	58.5100	135	58.5100
E08	20191027	0507	38	06.1700	136	15.9000
E07	20191027	0910	38	13.7060	136	32.5018
E06	20191027	1330	38	21.3500	136	49.8400
E05	20191027	1731	38	28.5800	137	07.1100
E04	20191027	1204	38	36.4864	137	24.1605
E03	20191028	0121	38	43.9200	137	41.2800
E02	20191028	0509	38	51.7200	137	58.4400
E01	20191028	0907	38	59.2066	138	15.4341
SI06	20191028	1721	39	20.0100	137	24.7800
SI05	20191028	2135	39	05.1536	137	34.7587
SI04	20191029	0157	38	50.3400	137	45.0100
SI03	20191029	0524	38	35.0700	137	55.2400
SI02	20191029	0954	38	20.9911	138	05.7013
SI01	20191029	1356	38	08.6800	138	13.1700
FATO1	20191030	0643	38	40.1900	137	51.8600
FATO2	20191031	0240	38	40.6165	137	52.4331

(5) Preliminary Results

a) YR-line

The current direction near the surface was varied counterclockwise (left panel of Figure 3.3.1). The cyclonic eddy around the Yamato basin affected the change of current direction. It is inferred that the cyclonic eddy depicted by SSH isoline is slightly shortened northeastward from this result. Southwestward current velocity was over 0.3 m s^{-1} in the offshore side of this line and northeastward current velocity was almost 0.3 m s^{-1} in the coastal side (middle and right panel of Figure 3.3.1).

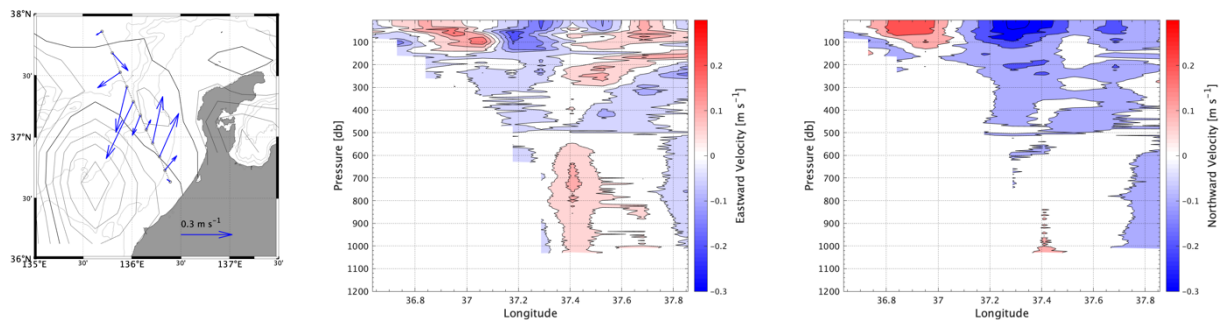


Figure 3.3.1: Velocity vector near the surface and SSH contour (left), vertical sections of eastward velocity

(middle) and northward velocity (right) along YR-line. Isoline on the left panel shows the horizontal distribution of ADT on October 24, 2019.

b) E-line

Two eddies existed from the SSH image in Figure 3.3.2 (left panel). Cyclonic eddy was distributed for more than 3 months and anti-cyclonic eddy was developed on mid-October inferred from SSH images. Current direction was varied anti-clockwise in the east of E-line and clockwise in the west of E-line along these eddies. Inside of the anti-cyclonic eddy, the velocity was over 0.3 m s^{-1} from the surface to around 300 m in depth. Besides, inside of the cyclonic eddy, the velocity was over 0.3 m s^{-1} from the surface to around 100 m in depth and the current structure was shallower than anti-cyclonic eddy (middle and right panel of Figure 3.3.2). The complex vertical structure of the current exists around the seamount around 137° E (middle panel of Figure 3.3.2). This result is assumed to be the topographic effect.

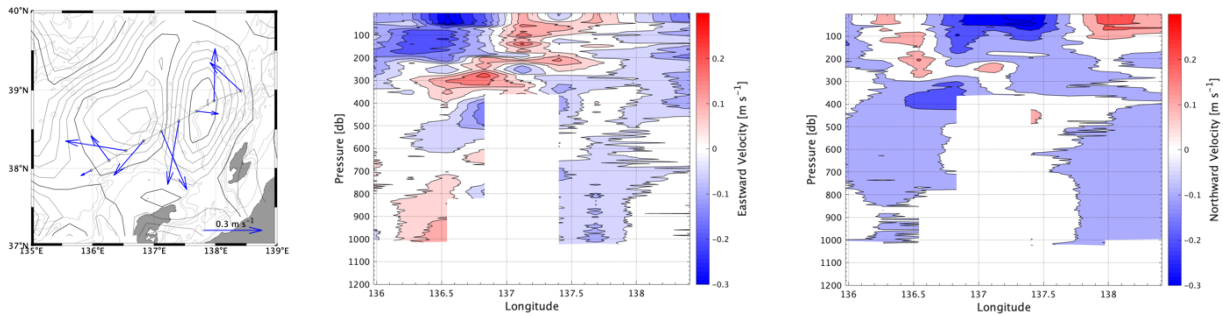


Figure 3.3.2: Velocity vector near the surface and SSH contour (left), vertical sections of eastward velocity (middle) and northward velocity (right) along E line. Isoline on the left panel shows the horizontal distribution of ADT on October 24, 2019.

c) SI Line

Northeastward current around 0.3 m s^{-1} was detected from the surface to around 150 m in depth near the Sado Islands. The counterclockwise variation of the current direction affected by the cyclonic eddy was seen from the left panel of Figure 3.3.3. In the lower layer under the cyclonic eddy, southward current was observed. The surface currents influenced by eddies are well corresponds with the current measured by S-ADCP and the geostrophic velocity derived from the CDT profiles in all three lines.

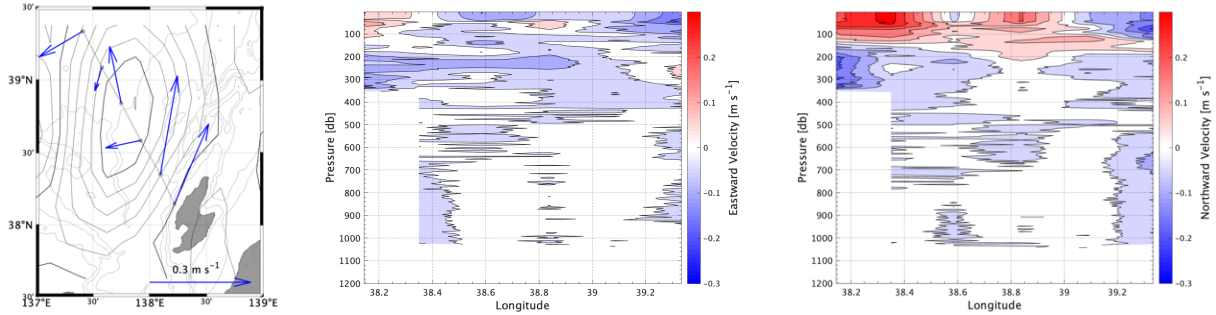


Figure 3.3.3: Velocity vector near the surface and SSH contour (left), vertical sections of eastward velocity (middle) and northward velocity (right) along SI line. Isoline on the left panel shows the horizontal distribution of ADT on October 24, 2019.

3.4 Buoy Deployment

(1) Personnel

Itsuka Yabe: AORI, principal investigator

Yusuke Kawaguchi: AORI

Taku Wagawa, Daiki Ito: FRA

Tomoharu Senjyu, Akie Sakai: RIAM

Kazuki Horio, Koshiro Taya: Hokkaido University

(2) Objectives

Six satellite-tracked buoys were deployed to examine the pathway of TWC jet and behavior of cyclonic and anti-cyclonic eddies.

(3) Instruments and methodology

The satellite-tracked buoys which constructed by holey sock drogue and SPOT were deployed on this cruise. SPOT is a GPS tracking device which gets the position data from GPS satellites and sends the position for communication satellite. We can check latitude and longitude data on the website. The all buoys transmitted their GPS positioning data every hour. The buoys' drogues were set at 50 m depth, below the surface mixed layer, in order to properly track the flow under the seasonal thermocline. Two of the buoys were deployed on the jet structure of TWC on the YR-line, and others were deployed within the eddies along the E-line.

(4) Buoy deployment positions

Buoy No.	Stn	Date	Time	Lat (deg)	Lat (min)	Lon (deg)	Lon (min)
1643	YR02	20191026	1215	36	43.7742	136	20.2260
2601	YR02	20191026	1235	36	44.2865	136	19.9069
3008	E06	20191027	1424	38	21.3237	136	49.6816
3109	E06	20191027	1435	38	21.9057	136	49.7010

3284	E02	20191028	0607	38	52.0456	137	58.5552
4330	E02	20191028	0617	38	52.3634	137	59.2825

(5) Preliminary Results

The positioning data of buoy No.1643 from October 26 to November 12 indicated that the pathway of TWC's coastal branch (Figure 3.3.4 upper left). The buoy traveled along the north of the Noto Peninsula and move toward the inside of the Toyama Bay. The buoy No.3008 and No.3109 went around the anti-cyclonic eddy about a week (Figure 3.3.4 upper right and lower left). The current velocity is almost 0.2 m s^{-1} . Flow directions changed clockwise and inertial oscillation with a period of 19 hours were shown from flow directions and velocities. It is assumed that the effect of atmospheric disturbance relates to this oscillation. The buoy No.3284 which deployed inside the cyclonic eddy shows the anti-clockwise trajectory and leaves from the eddy around the north of the Sado Islands. In this area, strong northeastward flow was observed from the CTD and LADCP measurement.

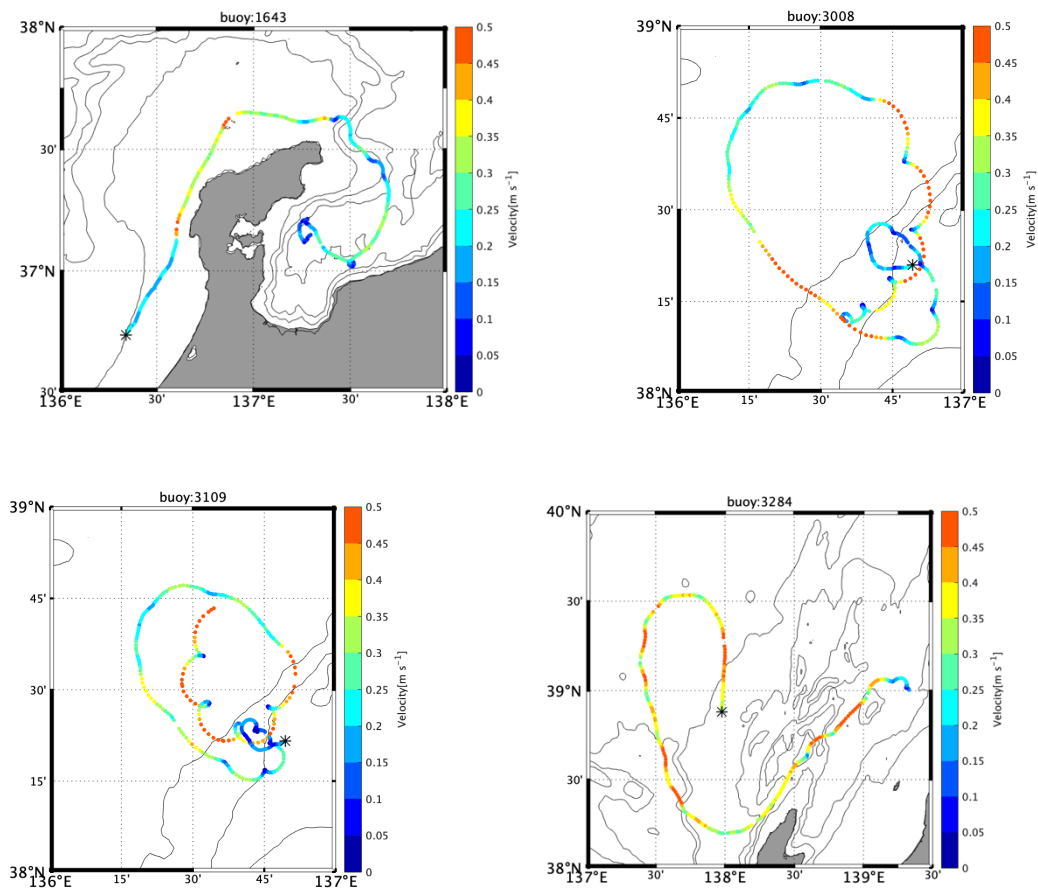


Figure 3.4.1: The trajectories of each buoy, No.1643, 3008, 3109 and 3284, respectively. Color of mark indicates current velocity and asterisk mark shows the first position data after deployment. Gray isolines show the bathymetry.

3.5. SADCP

(1) Personnel

Daiki Ito: FRA, principal investigator

Yusuke Kawaguchi, Itsuka Yabe: AORI

Taku Wagawa: FRA

Tomoharu Senjyu, Akie Sakai: RIAM

Kazuki Horio, Koshiro Taya: Hokkaido University

(2) Objectives

Current velocity was continuously observed by a shipboard acoustic Doppler current profiler (SADCP) to examine velocity structures along the ship track.

(3) Instruments and methodology

RDI 38-kHz SADCP was used. The corrected data were averaged into time bins of 5 min by intervals of 8 m and 16 m in depth during the former and latter period of the cruise, respectively. These data were calibrated for misalignment angle. Misalignment angle was estimated from the ship velocities measured by a Global Positioning System (GPS) and by bottom tracking ADCP data. Data with percent good (PG) $4 < 70$ were eliminated in the analysis.

(4) Preliminary Results

(a) Horizontal map

Horizontal velocity along the ship track (Fig. 3.5.1) was generally consistent with distribution of mesoscale eddies on the satellite sea surface height map produced by AVISO (<https://www.aviso.altimetry.fr>). Comparison of the horizontal velocity field at 50- and 200-m depth reveals that the current direction was almost the same between the two layers, but the magnitude of the velocity tended to be smaller at the 200-m depth than at the 50-m depth. Notable exceptions appeared around the western edge of anticyclonic eddy (38.2° N, 136.5° E) and the western edge of cyclonic eddy (38.75° N, 137.5° E). Relatively large horizontal velocity (~ 0.3 m s⁻¹) was extended to the deep layer in these two areas.

① YR-line

Southwestward velocity of approximately 0.3 m s⁻¹ and northeastward velocity of approximately 0.3 m s⁻¹ were observed western part (centered at 136° E) and eastern part (centered at 136.25° E) of YR-line, respectively (Fig. 3.5.2). YR-line was along the northeast of a meridionally-elongated cyclonic eddy (Fig. 3.5.1). The observed velocity reflected this eddy field. Above the bottom boundary in the nearshore (around 136.3° E), on the other hand, southwestward flow (0.2 m s⁻¹) was obvious.

② E-line

Along the E-line, velocity distribution was largely consistent with the distribution of mesoscale eddies (Fig. 3.5.1 and Fig. 3.5.3). An anticyclonic eddy was located at the western part of E-line and hence northwestward and southeastward flow were at around 136.5° E and 136.7° E, respectively. Another cyclonic eddy was distributed east of the anticyclonic eddy and resulting northward flow was at the eastern edge of E-line. As mentioned above, the northwestward flow at the western edge of the anticyclonic eddy (136.5° E) and the southeastward flow at the western edge of cyclonic eddy (137.5° E) extended to 300-m depth. Meanwhile, LADCP captured velocity inversion near the sill at around 137.2° E (Fig. 3.3.2 in Section 3.3). The northwestward flow was also recognized above the sill in the SADCP section (Fig. 3.5.3) though the structure is not clear compared with LADCP probably due to masking.

③ SI-line

SI-line crossed the cyclonic eddy perpendicular to E-line (Fig. 3.5.1). Velocity distribution corresponded to flow field generated by the cyclonic eddy (Fig. 3.5.4): southwestward and northeastward velocity of $0.2\text{--}0.3\text{ m s}^{-1}$ were in the western and eastern part of SI-line, respectively. Whereas LADCP observed velocity inversion near Sado island (Fig. 3.3.3 in Section 3.3), such structure was not found in Fig. 3.5.4.

④ XCTD-line

Zonal and meridional velocity sections during XCTD observation are illustrated in Fig. 3.5.5. This survey was conducted along E-line two days after the CTD and VMP observation. General structure was maintained in the two days (Fig. 3.5.3 and Fig. 3.5.5). Laterally extended northward flow below the surface southward flow were especially obvious at 100- to 300-m depth. Velocity inversion above the sill at around 137.2° E observed by LADCP (Fig. 3.3.3 in Section 3.3) was obvious in this section. Taking into consideration that a staircase-like density structure was observed by XCTD in this region (Fig. 3.6.1 in Section 3.6), this vertical velocity shear would contribute to mixing of water mass.

(b) Timeseries at FATO station

A continuous SADCP observation was conducted near FATO from 9:00 pm on October 29 to 5:00 pm on October 29 UTC (Fig. 3.5.6). Weak northwestward velocity ($\sim 0.1\text{ m s}^{-1}$) existed within the surface 200-m layer during the early part of the observation. During the latter part, on the other hand, weak northeastward flow ($\sim 0.1\text{ m s}^{-1}$) was observed at this station. Northward component of approximately 0.1 m s^{-1} gradually extended to deep layer: it was recognized within surface 50-m layer during the former period but within surface 200-m layer during the latter period.

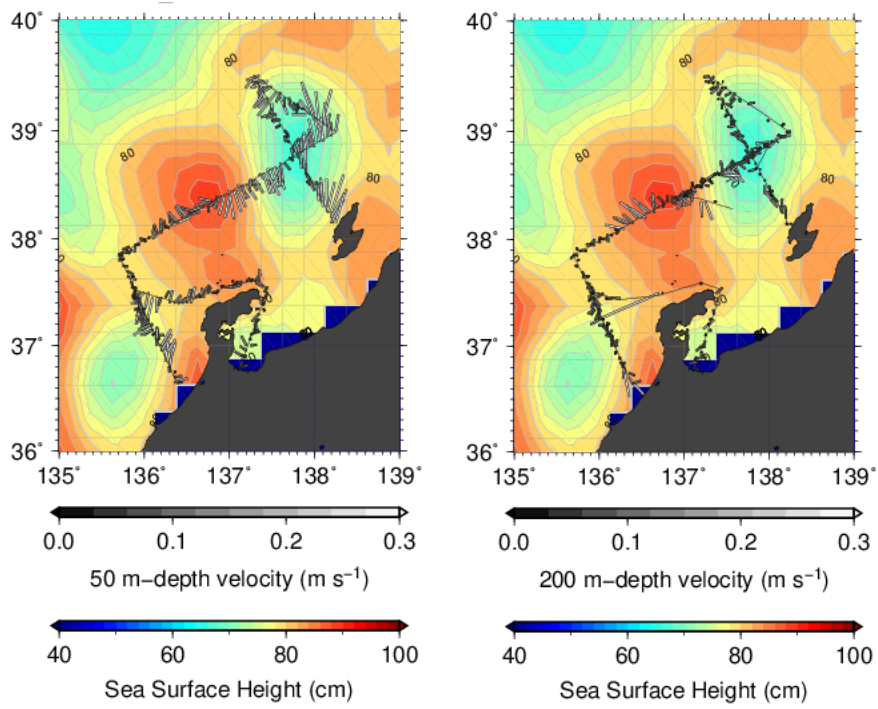


Figure 3.5.1: Horizontal velocity along the ship track (left) at 50- and (right) 200-m depth on Sea surface height map for October 29, 2019.

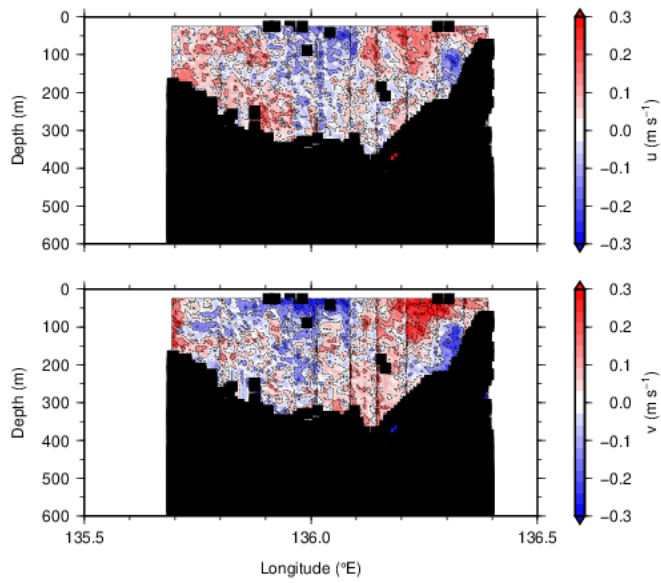


Figure 3.5.2: Sections of (top) zonal (positive eastward) and (bottom) meridional (positive northward) velocity along YR-line. Data with $PG\ 4 < 70$ are masked.

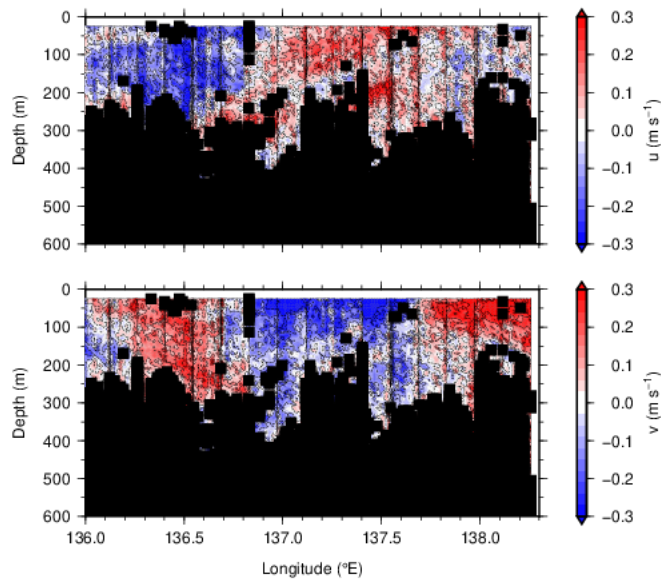


Figure 3.5.3: As Fig. 3.5.2, but for E-line.

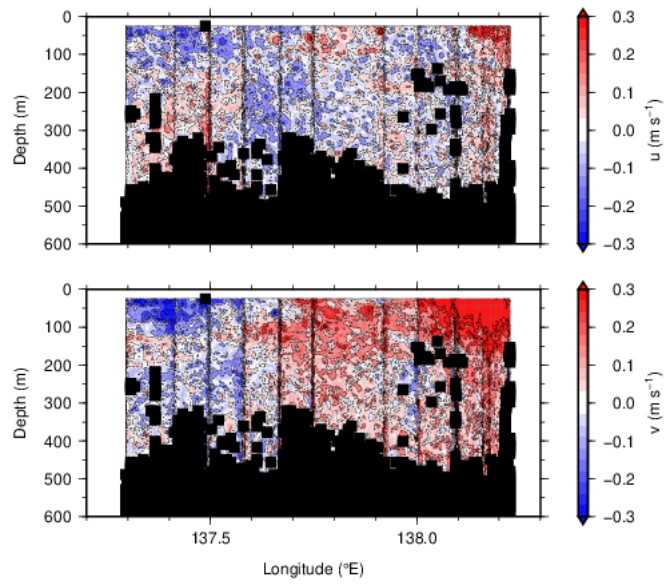


Figure 3.5.4: Same as Fig. 3.5.2 but for the SI-line.

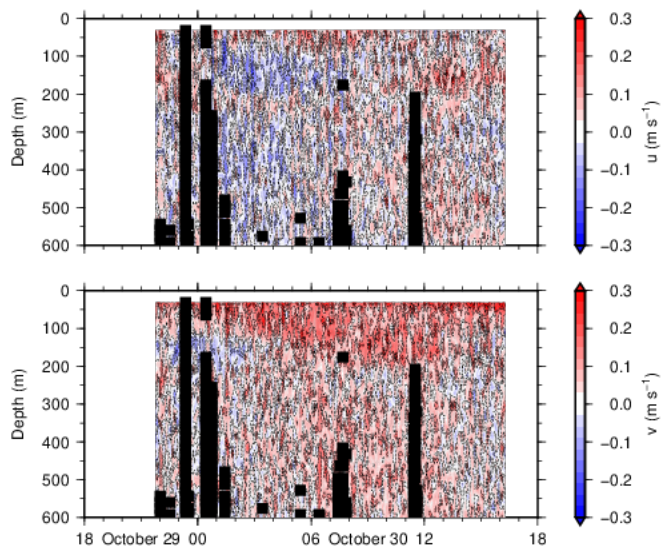


Figure 3.5.5: As Fig. 3.5.2, but for XCTD-line.

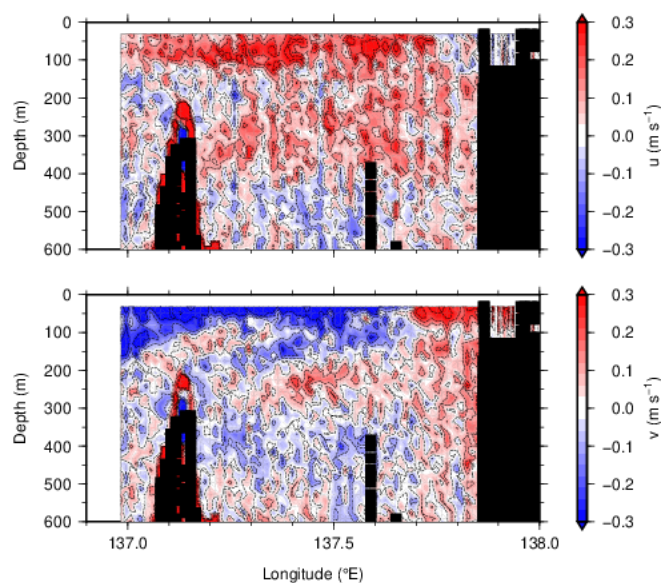


Figure 3.5.6: Timeseries of (top) zonal (positive eastward) and (bottom) meridional (positive northward) velocity observed at FATO. Data with $PG\ 4 < 70$ are masked.

3.6. XCTD

(1) Personnel

Daiki Ito: FRA, principal investigator

Yusuke Kawaguchi, Itsuka Yabe: AORI

Taku Wagawa: FRA

Tomoharu Senjyu, Akie Sakai: RIAM

Kazuki Horio, Koshiro Taya: Hokkaido University

(2) Objectives

Expendable conductivity-temperature-depth profiler (XCTD) observations were conducted along the E-line of CTD and VMP observation line in order to capture small-scale water mass structure in and around a cyclonic eddy.

(3) Instruments and methodology

This observation was carried out toward the center of a cyclonic eddy from its western edge on October 29, 2019 (Fig. 3.6.1). The cyclonic eddy was northeast of an anticyclonic eddy and several western stations were located inside the anticyclonic eddy. At each station an XCTD (Tsurumi Seiki Co. Ltd; XCTD-1 type) was deployed and temperature and salinity profile were obtained. The observation line had 15 stations and all the deployment were completed within 7 hours. Distance between stations was about 4.7 miles (~ 8.7 km). The vessel speed was 9 kt throughout the survey.

After applying 31-m Hanning filter to temperature and salinity data, potential temperature and

potential density were calculated from these profiles. They were interpolated onto a 1-m depth vertical grid using Akima spine (Akima, 1970).

(4) XCTD deployment positions

#	Stn.	Date (yyyymmdd)	Time (JST)	Latitude	Longitude
1	X15	20191029	21:57	38-25.2912N	136-58.5436E
2	X14	20191029	22:26	38-27.1682N	137-02.8022E
3	X13	20191029	22:56	38-29.0513N	137-07.0783E
4	X12	20191029	23:26	38-30.9343N	137-11.3390E
5	X11	20191029	23:56	38-32.8009N	137-15.6045E
6	X10	20191030	00:26	38-34.6727N	137-19.8720E
7	X09	20191030	00:56	38-36.5530N	137-24.1402E
8	X08	20191030	01:27	38-38.5091N	137-28.3750E
9	X07	20191030	01:57	38-40.3314N	137-32.6795E
10	X06	20191030	02:26	38-42.1940N	137-36.9677E
11	X05	20191030	02:55	38-44.0829N	137-41.2454E
12	X04	20191030	03:23	38-45.9725N	137-45.5035E
13	X03	20191030	03:51	38-47.9725N	137-49.7738E
14	X02	20191030	04:21	38-49.7287N	137-54.0656E
15	X01	20191030	04:50	38-51.6056N	137-58.3159E

(5) Preliminary Results

Shoaling of isopycnals was observed inside the cyclonic eddy (Fig. 3.6.2). For example, the difference in depth of the 26.8 kg m⁻³ isopycnal between the outside and the center of the cyclonic eddy was approximately 100 m: the depth of the isopycnal was 200 m at the westernmost station, which was located in the adjacent anticyclonic eddy, whereas that was 100 m at the center of the cyclonic eddy.

Patches of high salinity (~ 34.4) water with the horizontal scale of several tens of kilometers were between the 25.2 and 25.6 kg m⁻³ isopycnal surfaces (Fig. 3.6.2): these patches were centered at 137° E, 137.25° E, and 137.5° E. In the surface 50-m layer, on the other hand, low salinity (~ 33.6) water with the horizontal scale of approximately 20 km was at around 137.3° E, near the boundary of the anticyclonic and cyclonic eddy. Moreover, a staircase-like structure existed above the sill at around 137.1° E.

Reference

Akima, H., 1970: A new method of interpolation and smooth curve fitting based on local procedures. *J. Assoc. Comput. Math*, **17**, 589–602, doi:10.1145/321607.321609.

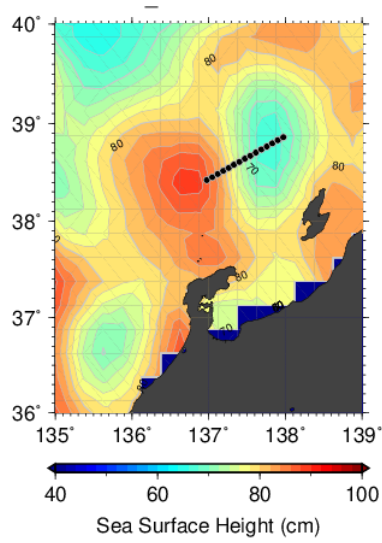


Figure 3.6.1: Positions of XCTD observations (black circle) on Sea surface height map for October 29, 2019.

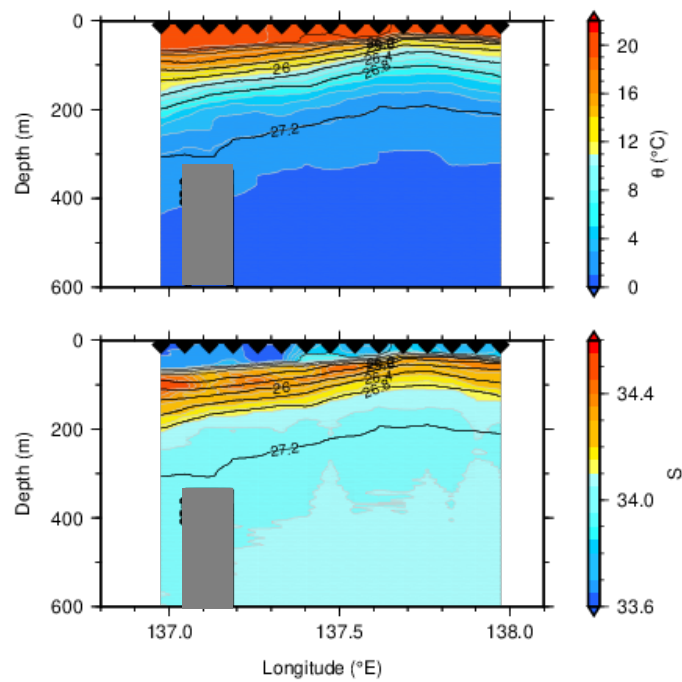


Figure 3.6.2: Hydrographic sections of (top) potential temperature and (bottom) salinity along the XCTD-line. Potential density is shown in black contour with a contour interval 0.4 kg m^{-3} . Black diamonds at the top of sections indicate XCTD station locations. Gray rectangle denotes the sill.

4. Notice on Using

All the data need careful treatment for calibrations, analysis and publish before public opening. For the data usage, please inquire the chief scientist for the details.

This cruise report is a preliminary documentation as of the end of cruise.

This report is not necessarily corrected even if there is any inaccurate description (i.e. taxonomic classifications). This report is subject to be revised without notice. Some data on this report may be raw or unprocessed. If you are going to use or refer the data on this report, it is recommended to ask the Chief Scientist for latest status.

Users of information on this report are requested to submit Publication Report to Cooperative Research Cruise office.

E-mail: kyodoriyo@aori.u-tokyo.ac.jp